Hindawi
Journal of Nanomaterials
Volume 2021, Article ID 2204776, 12 pages
https://doi.org/10.1155/2021/2204776

Research Article

Comparative Analysis of Nanosilver Particles Synthesized by Different Approaches and Their Antimicrobial Efficacy

Hala M. Abdelmigid,[1] **Maissa M. Morsi**,[2] **Nahed Ahmed Hussien**,[2] **Amal Ahmed Alyamani**,[1] **and Noha Moslah Al Sufyani**[2]

[1]*Department of Biotechnology, College of Science, Taif University, P.O. Box 11099, Taif 21944, Saudi Arabia*
[2]*Department of Biology, College of Science, Taif University, P.O. Box 11099, Taif 21944, Saudi Arabia*

Correspondence should be addressed to Nahed Ahmed Hussien; nahed199@gmail.com

Received 15 September 2021; Accepted 30 September 2021; Published 15 October 2021

Academic Editor: Thathan Premkumar

Silver nanoparticles (AgNPs) were extensively used in different fields worldwide. There is a continued increase in their productions to fulfill various uses. Biological and chemical AgNP syntheses were the most popular mechanisms in this field. Agrowastes are rich in proteins, phenolics, and flavonoids that could act as bioreductant agents in AgNP biological synthesis. The present study was aimed at synthesizing AgNPs via chemical and biological methods using trisodium citrate, pomegranate fruit peel, and coffee ground waste extracts. Moreover, silver nanoparticles were monitored by UV-vis spectroscopy and characterized using zeta potential, size distribution mean, scanning electron microscope (SEM), X-ray diffractometer (XRD), and Fourier transforms infrared spectroscopy (FTIR). Four pathogenic bacterial strains (*Enterobacter aerogenes*, *Klebsiella pneumoniae*, *Pseudomonas aeruginosa*, and MRSA) were used to assess the antimicrobial effect of the synthesized AgNPs (2, 4, and 8 mg/ml). Results report the successful formation of silver nanoparticles chemically (AgNPs_Chem) and biologically by using pomegranate peel extract (AgNPs_PPE) and coffee ground waste extract (AgNPs_CE) due to the change of color to dark brown that is confirmed by UV-vis sharp absorption spectra at specific wavelengths. Characterization using SEM and XRD revealed their crystalline shape with a mean size of AgNPs_Chem = 62.75, AgNPs_CE = 273.7 nm, and AgNPs_PPE = 591.9 nm. AgNPs_Chem show higher negativity of zeta potential (−46.7 mV) than AgNPs_CE (−12.6 mV), followed by AgNPs_PPE (−7.98 mV), which had the least stability. All the synthesized AgNPs show antimicrobial potential on all selected strains. However, 8 mg/ml shows the most effective concentration and has more efficiency on *K. pneumoniae* than others. Overall, the results highlight that the use of agrowastes could be an ecofriendly way to synthesize AgNPs biologically that have the same antimicrobial effect as the chemically synthesized AgNPs.

1. Introduction

Owing to the extensive applications of nanomaterials in various areas of industry, technology, and agriculture along with medicine, the worldwide request for nanomaterials is increasing exponentially. Due to the commercial consumption of silver nanoparticles (AgNPs) in various applications, the annual increase in AgNP production was estimated to be hundreds of tons worldwide [1]. In chemical preparation methods, producing stable colloidal AgNPs of desired sizes within the nanometer scale, apart from being an expensive chemical, can also generate oxidized species during the synthesis process, which cannot be easily separated from the nanomaterial product [2]. Such the undesirable chemical entities can significantly restrict the application opportunities as well as the biological compatibility of the produced nanomaterials.

Consequently, the utilization of nanomaterials must be complemented with innovative, low-cost, ecofriendly production processes, which reduce the use of hazardous chemicals and reduce the cohort of unsafe wastes [2, 3]. Green synthesis strategies of metal nanoparticles have been recently growing, as more safe alternatives to conventional chemical methods and low impact on the environment. Such

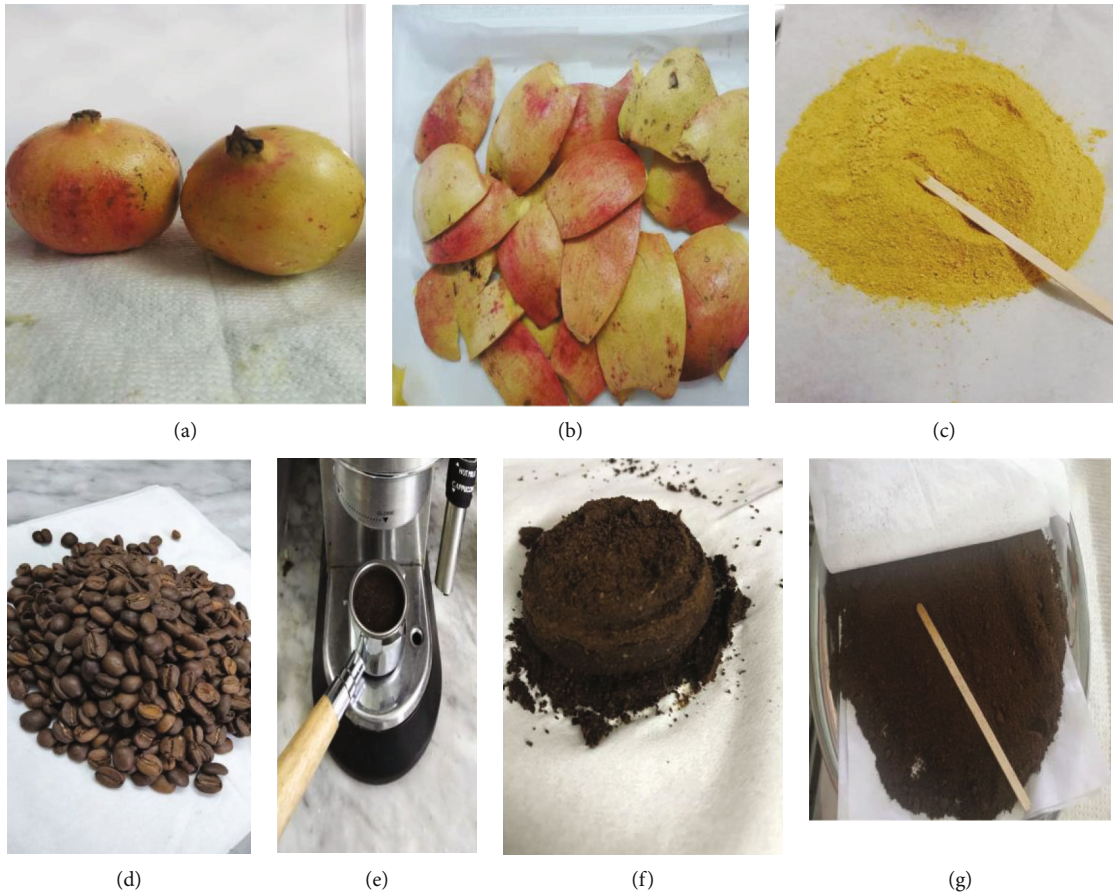

Figure 1: Steps of pomegranate peel (a–c) and coffee ground (d–g) waste collection.

approaches apply mild experimental conditions such as ambient temperature and pressure; require nontoxic, environmentally benign solvents, and reducing agents as well as capping materials [4]. They involve either living organisms, such as bacteria [5] or fungi [6]. Natural extracts [7] obtained from whole plants, extracts of different parts of plants, and fruit waste have been well applied for green nanomaterial synthesis. Plant extracts contain various metabolites (e.g., polysaccharides, proteins, vitamins, or alkaloids), which are generally nontoxic, biodegradable, and can act both as reducing and capping agents, thereby promoting the formation, and preventing the agglomeration of nanoparticles [2, 4, 8]. Application of plant- or fruit waste-based extracts could be more favorable due to a simple, cost-effective, and ecofriendly process relative to other biological paths of NP synthesis [9]. Nanoparticles have been effectively synthesized by a wide range of agrowastes such as Cocos nucifera coir, corn cob, fruit seeds and peels, wheat bran, rice bran, and palm oil mill effluent [10–16]. These agrowastes have been reported to be rich in biomolecules such as phenolics, flavonoids, and proteins, and that can serve as bioreductant agents in the green synthesis of diverse nanoparticles.

Pomegranate (*Punica granatum*) is one of the most important crops cultivated in Saudi Arabia. This fruit is rich in polyphenolic phytochemicals which have been shown to exhibit excellent antioxidant properties and therefore has been widely used in the food industry and in traditional medicine to treat various diseases is Saudi Arabia [17, 18]. The pomegranate peel is an agrowaste, which constitutes about 60% of the weight of pomegranate fruit. The pomegranate peel extract (PE) is also known for its high-nutrient content, consisting of minerals (e.g., potassium), vitamins, phenolics, flavonoids, antioxidants, and anticarcinogenic properties [19–21].

Coffee is one of the most popular beverages in the world that are commercially cultivated [22]. They are considered a rich source of biologically active compounds, especially polyphenols [23]. Its seeds (i.e., coffee beans) contain two types of alkaloids, caffeine and trigonelline, as major components. In addition to caffeine, there are adenine, xanthine, hypoxanthine, and guanine [24]. The coffee industry is responsible for the production of massive amounts of wastes [25]. Solid coffee ground (SCG) consists mainly of (hemi) cellulose, melanoidins, proteins, and polyphenols (lignins, tannins, and chlorogenic acids) [26]. Given the presence of organic components, Sunoqrot et al. [27] assumed that the polyphenol-rich aqueous extracts of arabica coffee beans represented by chlorogenic acids and melanoidins may produce nanostructures through oxidative coupling.

In this present work, biocompatible silver nanoparticles were synthesized via a variety of approaches using chemical and biological methods. Pomegranate fruit peel and coffee ground waste extracts have been used as capping and

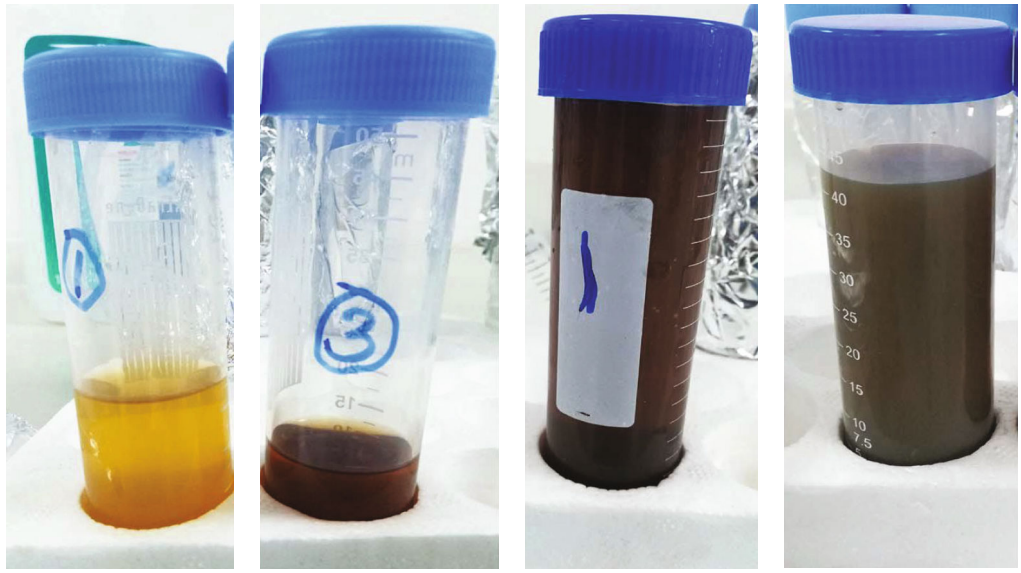

(a) (b) (c) (d)

Figure 2: Change of pomegranate peel extract (PPE) (a) and coffee ground extract (CE) (b) color due to silver nanoparticle AgNP_PPE (c) and AgNP_CE (d) preparations, respectively.

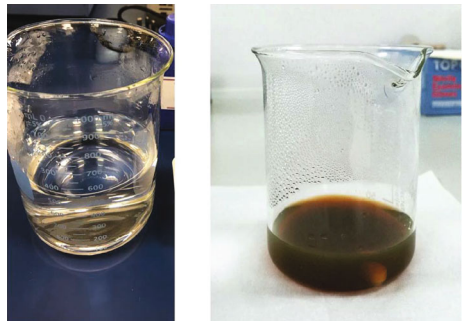

Figure 3: Preparation of silver nanoparticles by chemical reduction (AgNPs_Chem).

stabilizing agents for synthesizing silver nanoparticles from silver ions. The antimicrobial effect against pathogenic bacterial strains was measured, and an opportunity of their chemical versatility to load antimicrobial agents and surface ligands was taken.

2. Materials and Methods

2.1. Waste Collection and Preparation of Plant Extract. Fresh pomegranate (*Punica granatum L.*) fruits and coffee beans were purchased from local shop in Taif governorate, KSA. Pomegranate fruits were washed thoroughly using distilled water, and the seeds were then separated to obtain the peel. The isolated peels were oven dried at low temperature overnight until full dryness and ground into uniform coarse powder using a domestic blender.

Coffee beans were ground and used in preparing the coffee drink, and their waste was air dried at room temperature. Steps of pomegranate peel (PP) and coffee ground waste collection are briefly shown in Figure 1. For each waste product separately, 50 g powder was mixed with sterile distilled water (500 ml), boiled (10 min), filtered with Whatman filter paper, and cooled down at room temperature. Finally, pomegranate peel extract (PPE) and coffee ground extract (CE) were stored at 4°C for later use.

2.2. Green Synthesis of Silver Nanoparticles. Aqueous solution of silver nitrate ($AgNO_3$, 10^{-3} M, Alfa Aeser, UK) was mixed with each waste plant extract (PPE and CE) with ratio 9 : 1. Mixture was heated at 80°C with continuous stirring until change of extract color from pale yellow (PPE)/pale brown (CE) to dark brown, which refers to Ag nanoparticle (AgNP) formation (Figure 2). To obtain synthesized AgNPs, mixtures were centrifuged at 15000 rpm for10 min, supernatant was discarded, and the pellet was washed with sterile distilled water (3x) and centrifuged to get rid of any adsorbed substances on nanoparticles' surfaces. Biosynthesized silver nanoparticles (AgNPs_PPE and AgNPs_CE) were oven dried (60°C) overnight in glass petri dishes and then scraped out for further evaluations [28].

2.3. Chemical Synthesis of Silver Nanoparticles. Silver nanoparticles were prepared through chemical reduction according to Fang et al. [29]. 50 ml of 10^{-3} M $AgNO_3$ was boiled followed by gentle addition of trisodium citrate (1%, 5 ml, Sigma-Aldrich, Milan, Italy). Solution was heated with vigorous stirring until its color change from colorless to pale brown color (Figure 3). Chemical synthesized silver nanoparticles (AgNPs_Chem) were collected by centrifugation and dried as previously done with biologically prepared AgNPs_PPE and AgNPs_CE.

2.4. Characterization of Silver Nanoparticles

2.4.1. UV-Vis Spectroscopy. The absorption spectra of the synthesized silver nanoparticles (AgNPs_PPE, AgNPs_CE, and AgNPs_Chem) were measured in their aqueous form,

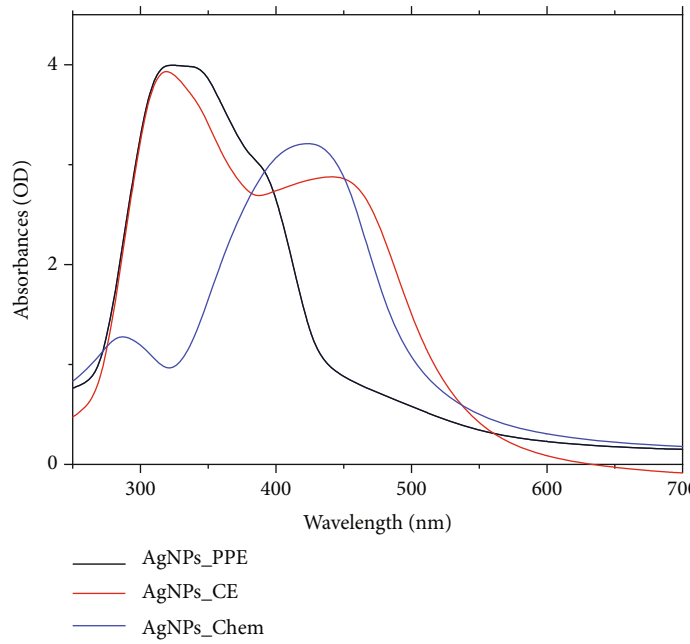

Figure 4: UV-visible spectral analysis of green synthesized AgNPs_PPE and AgNPS_CE and chemically synthesized AgNPs_Chem.

before dryness, using a UV-vis-NIR spectrophotometer (UV-1601, Shimadzu, Japan), using wavelength range from 200 to 800 nm. Autoclaved distilled water was used as a reference in measurement.

2.4.2. Size Distribution and Zeta Potential. The average size and surface charge of all synthesized silver nanoparticles were evaluated by using a particle size analyzer (Zetasizer Nano ZS, Malvern Instruments Ltd., UK) at 25°C with a detection angle 90°. All powder samples were freshly resuspended in 0.9% saline solution and sonicated for 30 mins at high speed before assessment to prevent nanoparticle aggregations.

2.4.3. Surface Morphology. Silver nanoparticles AgNPs_PPE, AgNPs_CE, and AgNPs_Chem (dried powder) were separately coated with gold using a Cressington Sputter Coater (108 Auto, thickness controller MTM-10, UK) for 10 mins prior to scanning. Scanning electron microscope (SEM, JEOL JSM-639OLA, Analytical Scanning Electron Microscope, Tokyo, Japan, that is present in the Electron Microscope Unit of Taif University) at 20 kV was used with different magnifications of ×500, ×2000, and ×3000 with scale bars of 50 μm, 10 μm, and 5 μm, respectively, to determine surface morphology. The X-ray diffractometer (XRD, Pan Analytical, X-pert pro, Netherland) was used to confirm the surface crystalline shape of the synthesized nanoparticles. XRD was used at 30 kV and 100 mA, and the spectrum was recorded by CuKα radiation with a wavelength of 1.5406 Å in the 2θ (from the range of 20°-80°). Patterns of XRD were plotted by the software OriginLab and compared with JCPDS card no. 040783.

2.4.4. Fourier Transforms Infrared Spectroscopy (FTIR). FTIR spectroscopy (Agilent Technologies, Santa Clara, CA, USA) was used to detect the possible functional groups found in PPE, CE, and sodium citrate (at wavelength range between 450 and 4000 cm^{-1}) that are responsible to silver nanoparticle synthesis and stabilization.

2.5. Agar Well Diffusion Assay. The antibacterial potential of silver nanoparticles (AgNPs_PPE, AgNPs_CE, and AgNPs_Chem) was evaluated by well diffusion method. Inhibition zones were recorded in millimeters (mm). Briefly, plates of the Mueller-Hinton agar were inoculated with five different pathogenic bacterial strains, separately: *Enterobacter aerogenes*, *Klebsiella pneumoniae* (*K. pneumoniae*), *Pseudomonas aeruginosa*, and methicillin-resistant *Staphylococcus aureus* (MRSA). Wells with a diameter of 7 mm were cut using sterile blue tips. For each plate, five wells were cut for plant extract, antibiotic, and three different concentrations of AgNPs. 100 μl of plant extract (PPE/CE) and 100 μl of the antibiotic ciprofloxacin 750 (1.6 mg/ml) were added as reference and positive control, respectively. Different concentrations (2 mg/ml, 4 mg/ml, and 8 mg/ml) of each silver nanoparticle were suspended in distilled water and were properly sonicated. 100 μl for each treatment and concentration were added per well. Plates were incubated at 37°C overnight. After incubation, diameters of the inhibition zone were measured by using a standard metric ruler.

2.5.1. Statistical Analysis. Data were expressed as the mean ± standard error (M ± SE). Statistical analysis was conducted using one-way ANOVA to differentiate between the inhibition zone diameter of different bacterial strains groups within the same AgNP treatment using GraphPad software (GraphPad®, 2017), in which, $***$ indicates $P \leq 0.001$, $**$ indicates $P \leq 0.01$, $*$ indicates $P \leq 0.05$, and ns (nonsignificant) means $P > 0.05$.

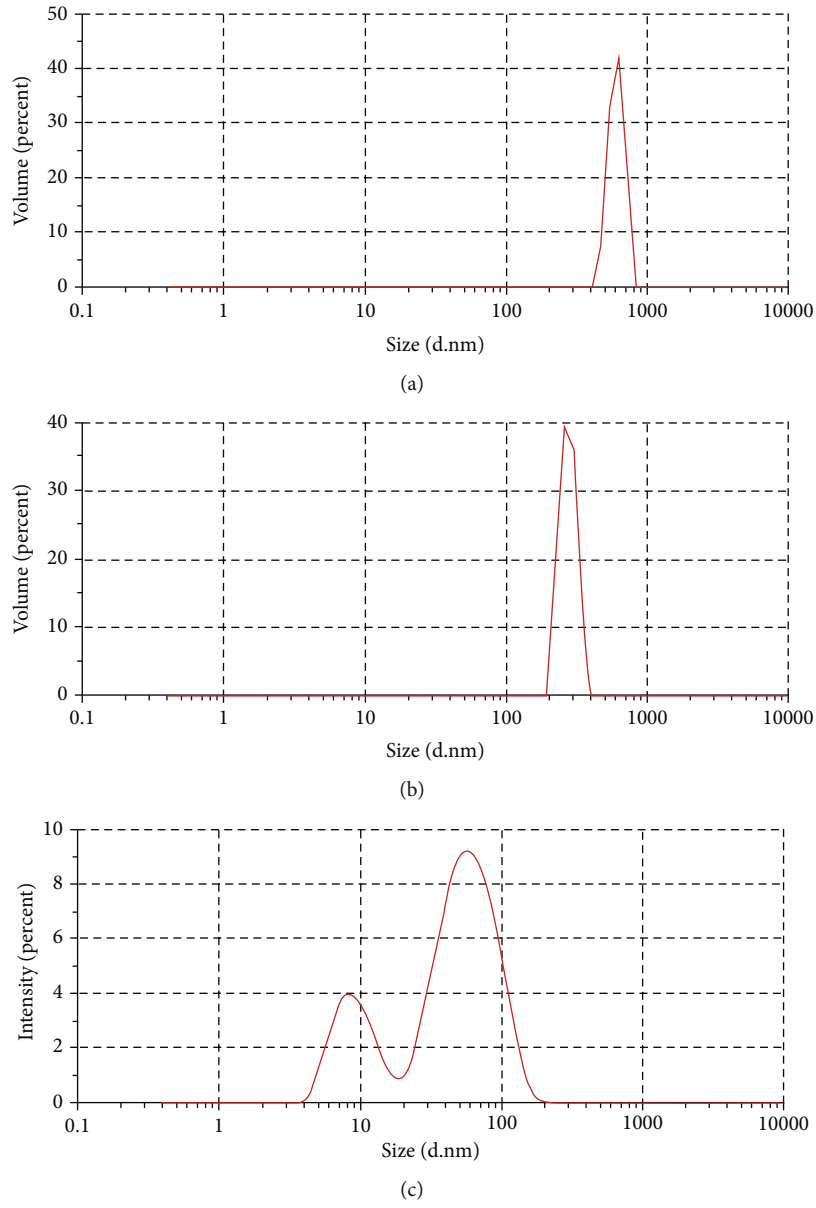

Figure 5: Average size of green synthesized (a) AgNPs_PPE (591 nm), (b) AgNPs_CE (273.7 nm), and chemically synthesized (C) AgNPs_Chem (62.68 nm).

3. Results and Discussion

3.1. Characterization of Silver Nanoparticles

3.1.1. UV-Vis Spectroscopy. The change of PPE, CE, and trisodium citrate colors from pale yellow, brown, and colorless, respectively, to dark brown color after $AgNO_3$ addition indicates successful formation of silver nanoparticles (Figures 2 and 3). The present results are in consistent with Jabir et al. [15]; they have reported color change of *Annona muricata* peel extract from deep yellow to dark brown due to the green synthesis of silver nanoparticles. AgNP_PPE, AgNP_CE, and AgNP_Chem syntheses were confirmed by UV absorbance because it is the simplest way to confirm colloidal metal nanoparticle formation due to their high surface plasmon resonances (SPR) [30, 31]. Figure 4 shows UV-vis sharp absorption spectra of AgNPs_PPE (350 nm), AgNPs_CE (2 sharp peaks at 320 nm and 440 nm), and AgNPs_Chem (430 nm) that typically detected previously for colloidal silver nanoparticles within the range from 350 to 600 nm [16, 32, 33]. The formed AgNPs have different UV spectra, due to different physical characteristics of formed silver nanoparticles, including size and shape, that affect their SPR [34].

The present study was consistent with previous reports, which recorded AgNP synthesis due to reduction of Ag^+ to Ag^0 in the presence of UV-vis spectroscopy using PPE, spent coffee ground extracts, and trisodium citrate at SPR 421 nm, 405–430 nm, and 420 nm, respectively [35–37]. It was known that SPR peak shifting towards a higher wavelength is accompanied by a decrease in the prepared AgNP size that is reported in the present study [38].

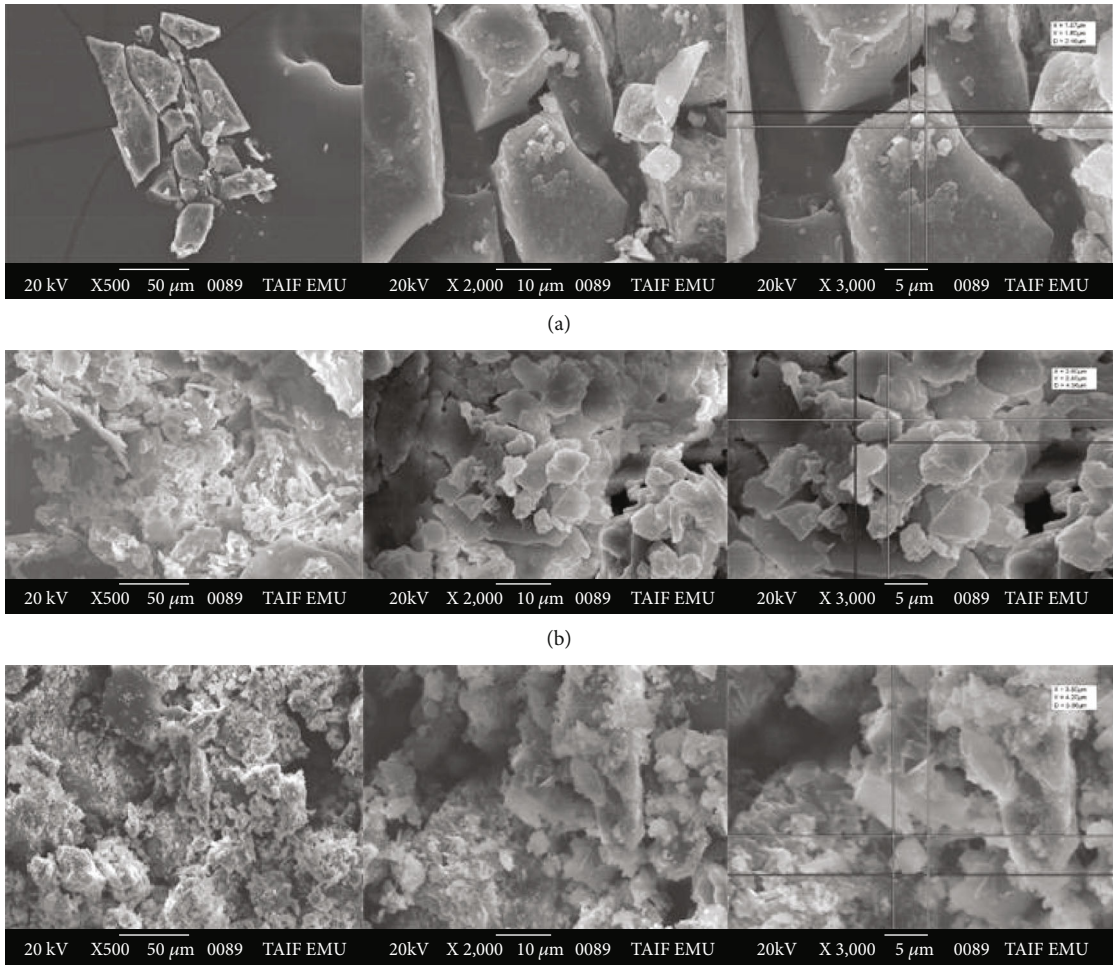

Figure 6: Scanning electron microscope photos showing the crystalline shape of AgNPs_PPE (a), AgNPS_CE (b), and AgNPs_Chem (c) with different magnifications.

3.1.2. Size Distribution and Zeta Potential. Zeta potential was used to estimate the stability of the synthesized AgNPs, in which an increase in positivity/negativity of zeta potential means a more stable nanoparticle. It was recorded that chemically synthesized AgNPs (−46.7 mV) were more stable than AgNPs_CE (−12.6 mV) followed by AgNPs_PPE (−7.98 mV) which had the least stability. Previously, it was reported that a high negative potential value increases nanoparticles' repulsion force that in turn helps in their dispersal, stability, and good colloidal nature [39]. AgNP stability affects their size, in which less stability initiates particle aggregation and in turn increased their size as reported in the present study with AgNPs_PPE = 591.9 nm, AgNPs_CE = 273.7 nm, and AgNPs_Chem = 62.75 nm (Figure 5). It was clear that chemically synthesized silver nanoparticles were more stable than biologically synthesized, and AgNPs synthesized from CE were more stable than those formed from PPE extracts. Therefore, AgNPs_Chem revealed the smallest size followed by AgNPs_CE and AgNPs_PPE.

The present results were incompatible with previous studies, in which AgNPs synthesized from PPE (31.6 nm; 118.6–231.7 nm), CE (21–255 nm), and trisodium citrate (5–10 nm) showed smaller size [35, 37, 40, 41]. It was known that change of $AgNO_3$ concentration and/or pH affects the size of synthesized silver nanoparticles. pH is inversely proportional to AgNP size, where at alkaline pH, the reaction rate increases with successive crystallization into smaller particles. Increasing pH reduces the aggregation tendency of nanoparticles due to complete surface charging and in turn increases their repulsion. In addition, increasing silver nitrate concentrations (1 mM to 5 mM) decreased the size of formed AgNPs as previously reported [38].

3.1.3. Scanning Electron Microscope (SEM) and XRD Analysis. Figure 6 shows the crystalline shape of biologically synthesized AgNPs_PPE and AgNPs_CE and chemically synthesized AgNPs_Chem by using SEM. This was confirmed by XRD evaluation, in which four main standard peaks were reported according to Bragg's reflection of silver nanoparticles that indicates the face-centered cubic (FCC) crystalline shape. Those four main peaks were present at 2 $\theta = 38.3^{\circ}$, 44.49°, 64.6°, and 77.5° that corresponds to Ag planes 111, 200, 220, and 311, respectively (Figure 7). FCC crystalline shape was previously reported in silver

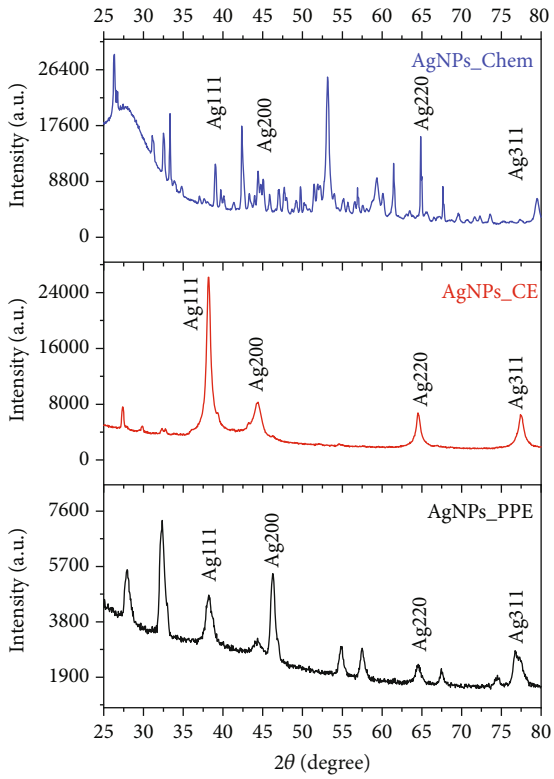

Figure 7: XRD patterns of AgNPs_PPE, AgNPs_CE, and AgNPs_Chem that confirm their crystalline shapes.

nanoparticle synthesis using various plant extracts as well as trisodium citrate as the chemical approach [19, 42–44]. The presence of other unpredicted diffraction peaks of AgNPs_PPE at 2θ of 27.90°, 32.38°, 46.43°, 55.00°, 57.00°, and 67.00° may be related to phytochemicals present in PPE. However, unassigned crystalline peaks at 2θ of 32.38° and 46.43° were also reported in previous studies [45, 46].

3.1.4. FTIR Evaluation of AgNPs. FTIR analysis was conducted to identify the possible biomolecules present in PPE, and the CE extract that are responsible for capping of silver nanoparticles, reduction, and stabilization. Figure 8 shows differences between each synthesized AgNP with its reference. Any change in sharpness or position of any peak is referred to group contribution in silver nanoparticles' synthesis. As reported earlier, AgNPs_PPE different peaks showed higher sharpness compared to PPE only. The recorded sharp peak at 2927 cm^{-1} was referred to C–H stretching; 1641 cm^{-1} was referred to C–O stretching vibration in quinine; 1351 cm^{-1} to C=C aromatic ring; 1228 cm^{-1} to C–O stretching in ether, ester, or phenol; and 1055 cm^{-1} to C–N stretching of the aliphatic primary amine [47]. Regions at 1315–1037 and 1456–1600 cm^{-1} were referred to phenolic groups participating in ion replacement response of flavanones' plant extract [48]. Therefore, flavonoids present in PPE are responsible for Ag^{+} to Ag^{0} reduction, capping, and stability of AgNPs [49]. Shankar et al. [50] had suggested that flavanones of plant extract might be adsorbed on the metal nanoparticle surface and determined by strong bands at 1074 cm^{-1}. PPE has different constituents including flavonols, gallotannins, quercetin, ellagic acid derivatives, catechins, procyanidins, and kaempferol that aid in its efficacy [51].

FTIR analysis of AgNPs_CE shows different sharp peaks in comparison to its extract CE. The AgNP_CE FTIR pattern shows a broad band at 3600–3000 cm^{-1}, two sharp peaks at 2922 cm^{-1} and 2852 cm^{-1}, and band at 1741 cm^{-1} due to –N-H and –O-H stretching vibrations, C–H bond asymmetric stretching of the methyl (–CH3) group, and C=O vibration, respectively. Peaks at the range from 1700 cm^{-1} to 1500 cm^{-1} may be assigned to C–C and C–N stretching vibration. Vibrations of different bonds such as -C-H, -C-O, and -C-N were determined in wavelength from 1400 cm^{-1} to 900 cm^{-1}. All assigned bands or peaks were previously reported in literature data that confirmed the presence of CO, OH, and NH_2 groups in CE [52, 53]. Those different groups of CE that are found in its constituents (hemicellulose, melanoidins, proteins, and polyphenols) might share in AgNP synthesis, capping, and stabilization [26].

In AgNP_Chem synthesis, trisodium citrate acts as a reducing agent. As previously reported, different peaks were assigned that might be referred to C–H stretching deformation (1282 cm^{-1}), nitro compound (NO) as NO_2 (1402 cm^{-1}), and C=O stretching asymmetric in COO– (1582 cm^{-1}), while an amine stretching appeared at higher wavelength at 3312 cm^{-1} [54, 55].

3.2. Antibacterial Activity Assay. Plant extracts (PPE and CE) and green and chemical synthesized AgNPs (AgNPs_PPE, AgNPs_CE, and AgNPs_Chem, respectively) were examined for their antimicrobial activity by using a well diffusion method. After 24 h incubation at 37°C, PPE and CE extracts did not show any inhibition on different bacterial strains. However, different concentrations of AgNPs (2 mg/ml, 4 mg/ml, and 8 mg/ml) suppress bacterial growth that appears as an inhibitory zone (Figure 9). Growth of the inhibitory zone increased by increasing AgNP concentration; 8 mg/ml shows the highest zone. In addition, Gram-negative bacteria *K. pneumoniae* show a higher zone inhibition in comparison to other Gram-negative bacteria (*Enterobacter aerogenes* and *Pseudomonas aeruginosa*) and the Gram-positive bacteria MRSA (Figure 10). There is no significant difference between the antibacterial potentials of the three different AgNP treatments on the selected bacterial strains.

Our results are consistent with Rautela et al. [56], in which they have reported antimicrobial effect of green synthesized AgNPs using *Tectona grandis* seed extracts on *Staphylococcus aureus*, *Bacillus cereus*, and *E. coli*. Also, they have recorded a higher inhibition zone on Gram-negative bacteria (*E. coli*) in comparison to Gram-positive bacteria (*B. cereus* and *S. aureus*) at the same concentration of AgNPs. Sensitivity of Gram-negative bacteria towards AgNPs compared to Gram-positive bacteria could be explained by variation in their cell wall composition. The cell wall of Gram-positive bacteria consists of a thicker peptidoglycan layer than that of Gram-negative bacteria. This leads to a more rigid structure that in turn increases difficulties towards AgNP penetration

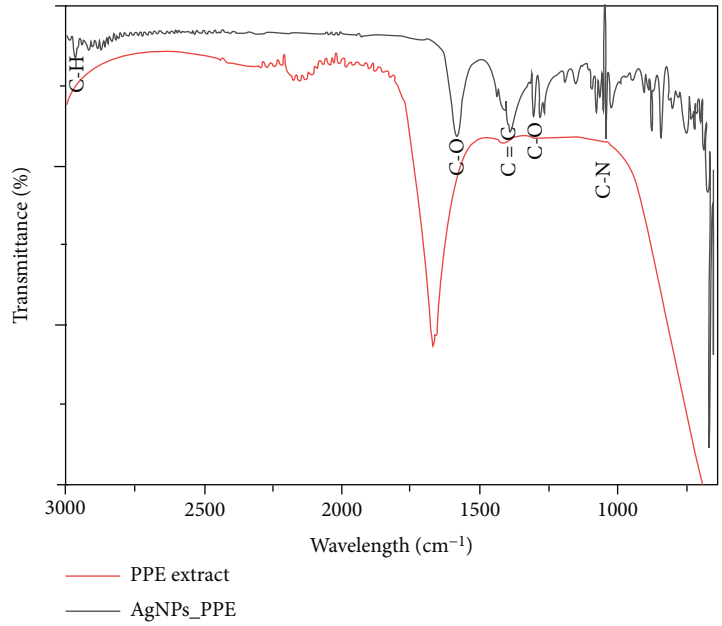

(a)

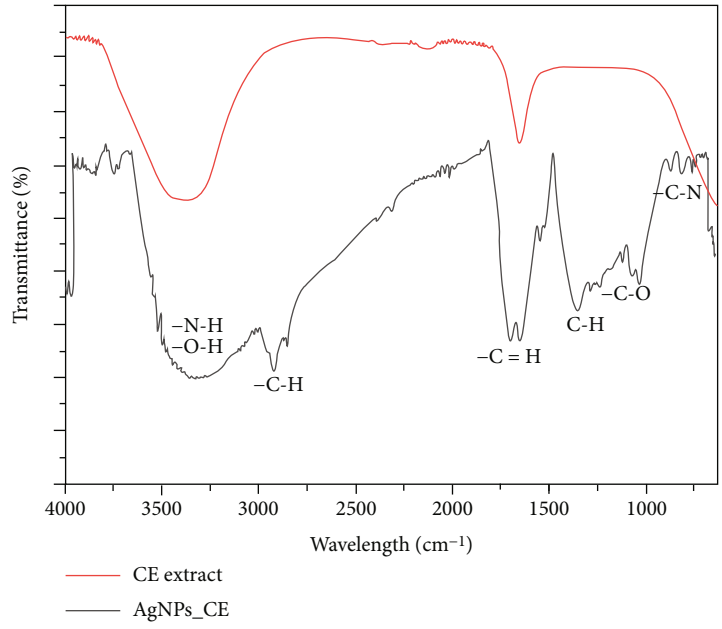

(b)

Figure 8: Continued.

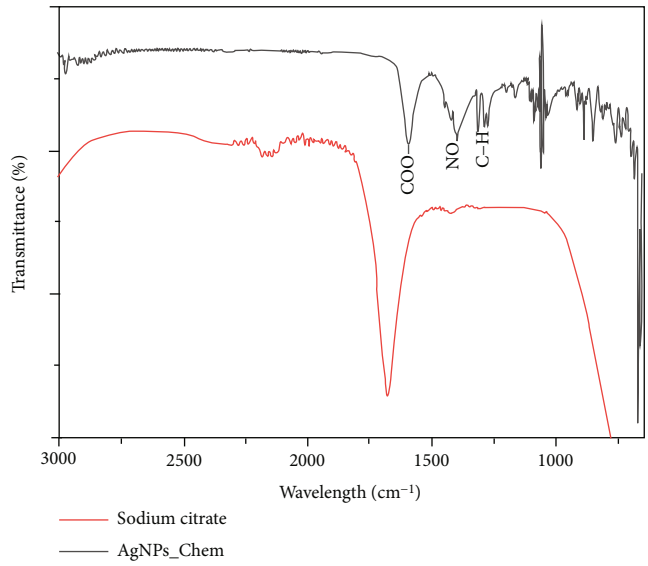

(c)

Figure 8: FTIR spectra of synthesized silver nanoparticles in comparison with their standard, in which (a) represents difference between AgNPs_PPE and PPE extract and (b) represents difference between AgNPs_CE and CE extract, while (c) shows difference between chemically synthesized AgNPs_Chem and sodium citrate.

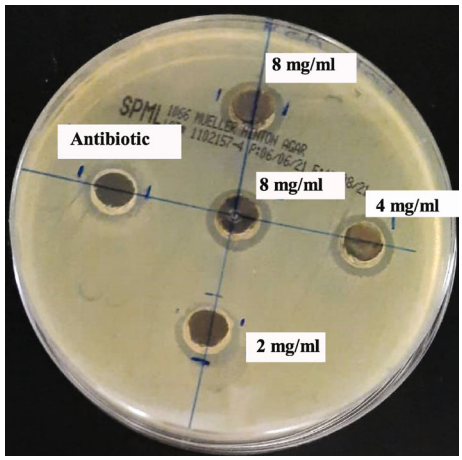

(a)

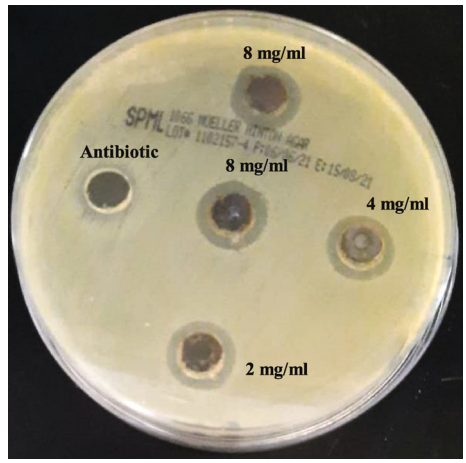

(b)

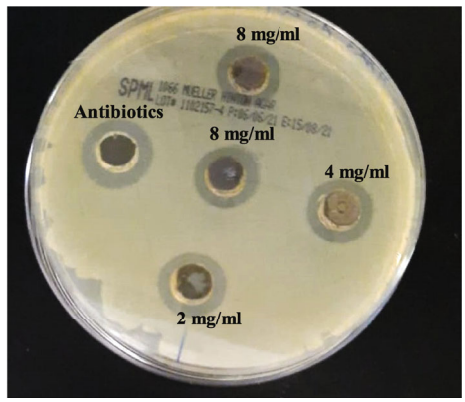

(c)

Figure 9: Representative photographs of silver nanoparticles (AgNPs) (2, 4, and 8 mg/ml) antimicrobial potential on different bacterial cells that show inhibition zones; *Enterobacter aerogenes* (a), *Pseudomonas aeruginosa* (b), and MRSA (c).

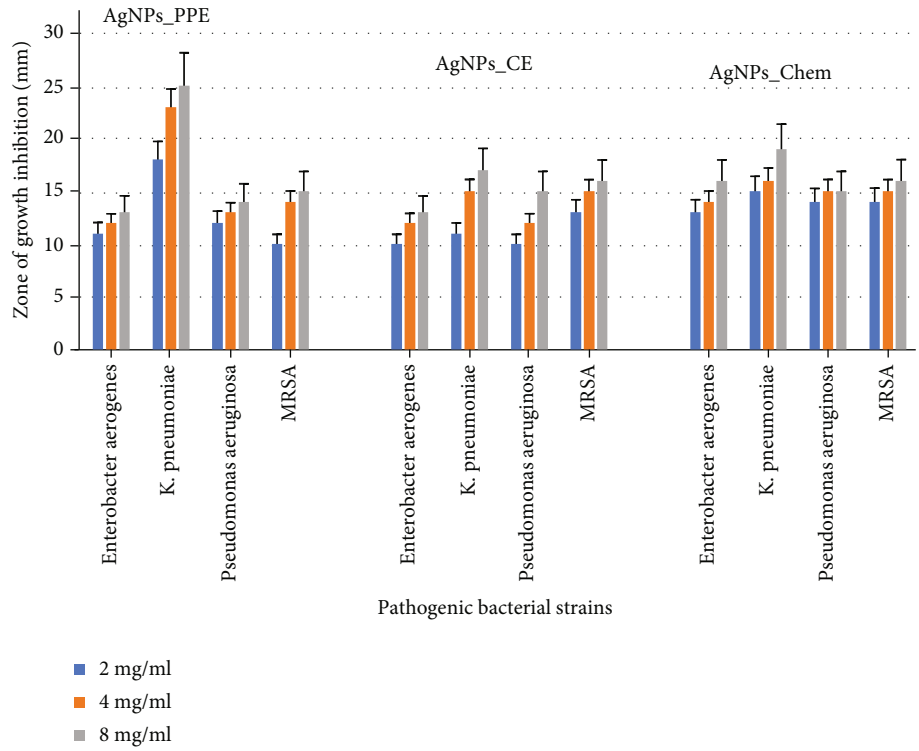

Figure 10: Antibacterial effect of biologically synthesized AgNPs_PPE, AgNPs_CE, and chemically synthesized AgNPs_Chem on different pathogenic bacterial strains *Enterobacter aerogenes*, *K. pneumoniae*, *Pseudomonas aeruginosa*, and MRSA. All groups within the same AgNP treatment were statistically nonsignificant (ns) in comparison with each other with means $P > 0.05$.

[57]. It is still unclear about the action of the mechanism of AgNPs on the bacteria. Rautela et al. [56] suggested that AgNPs could enhance the permeability of the membrane, by increasing sugar and protein leakage from the cytoplasm.

4. Conclusion

In the present study, we have provided a green, simple, and economic method for silver nanoparticle synthesis with the help of pomegranate peel and coffee ground extracts. In addition, a chemical reduction method was used for AgNP synthesis by the help of trisodium citrate. AgNP_PPE, AgNP_CE, and AgNP_Chem syntheses were confirmed by UV-vis spectroscopy at different absorbance. Zeta potential reports that chemically synthesized AgNPs were more stable than biologically synthesized AgNPs_CE and AgNPs_PPE that in turn affect their nanosize. XRD and SEM elucidated their crystalline shape, while FTIR determined different groups that might participate in capping and stabilization of silver nanoparticles. Green and chemical synthesized silver nanoparticles showed antibacterial activity which was investigated by the agar well diffusion method against different pathogenic strains. Further experiments are required for cytotoxic and genotoxic evaluation of the synthesized AgNPs and if there are any potential human risks for their application. In addition, large scales might be applied especially for the biological methods using different biological waste products.

Data Availability

All the data used to support the findings of this study are included within the article.

Conflicts of Interest

The authors declare that they have no conflicts of interest.

Authors' Contributions

All authors have participated in the practical part and data analysis. All authors have participated in writing the manuscript and have accepted the final version.

Acknowledgments

The authors are grateful to the Deanship of Scientific Research, Taif University, for providing research facilities and support. The authors also acknowledge the Department of Chemistry, College of Science for UV-Vis Spectroscopy and XRD Analysis. Staff of the electron microscopy unit is also acknowledged for assistance with SEM imaging. Special thanks are due to High Attitudes Research Centre, for providing facilities and equipment. This work was financially supported by a research project no. [1/441/130] from the Scientific Research Deanship at Taif University (institutional funding).

References

[1] L. Ge, Q. Li, M. Wang, J. Ouyang, X. Li, and M. M. Xing, "Nanosilver particles in medical applications: synthesis, performance, and toxicity," *International Journal of Nanomedicine*, vol. 9, pp. 2399–2407, 2014.

[2] G. Kozma, A. Ronavari, Z. Konya, and A. Kukovecz, "Environmentally benign synthesis methods of zero-valent iron nanoparticles," *ACS Sustainable Chemistry & Engineering*, vol. 4, no. 1, pp. 291–297, 2015.

[3] V. K. Sharma, R. A. Yngard, and Y. Lin, "Silver nanoparticles: green synthesis and their antimicrobial activities," *Advances in Colloid and Interface Science*, vol. 145, no. 1-2, pp. 83–96, 2009.

[4] K. B. Narayanan and N. Sakthivel, "Green synthesis of biogenic metal nanoparticles by terrestrial and aquatic phototrophic and heterotrophic eukaryotes and biocompatible agents," *Advances in Colloid and Interface Science*, vol. 169, no. 2, pp. 59–79, 2011.

[5] R. Joerger, T. Klaus, and C. G. Granqvist, "Biologically produced silver-carbon composite materials for optically functional thin-film coatings," *Advanced Materials*, vol. 12, no. 6, pp. 407–409, 2000.

[6] A. Boroumand Moghaddam, F. Namvar, M. Moniri, P. Tahir, S. Azizi, and R. Mohamad, "Nanoparticles biosynthesized by fungi and yeast: a review of their preparation, properties, and medical applications," *Molecules*, vol. 20, no. 9, pp. 16540–16565, 2015.

[7] A. K. Mittal, Y. Chisti, and U. C. Banerjee, "Synthesis of metallic nanoparticles using plant extracts," *Biotechnology Advances*, vol. 31, no. 2, pp. 346–356, 2013.

[8] S. Patra, S. Mukherjee, A. K. Barui, A. Ganguly, B. Sreedhar, and C. R. Patra, "Green synthesis, characterization of gold and silver nanoparticles and their potential application for cancer therapeutics," *Materials Science & Engineering. C, Materials for Biological Applications*, vol. 53, pp. 298–309, 2015.

[9] G. D. Saratale, R. G. Saratale, D. S. Kim, D. Y. Kim, and H. S. Shin, "Exploiting fruit waste grape pomace for silver nanoparticles synthesis, assessing their antioxidant, antidiabetic potential and antibacterial activity against human pathogens: a novel approach," *Nanomaterials*, vol. 10, no. 8, p. 1457, 2020.

[10] P. P. Gan, S. H. Ng, Y. Huang, and S. F. Y. Li, "Green synthesis of gold nanoparticles using palm oil mill effluent (POME): a low-cost and eco-friendly viable approach," *Bioresource Technology*, vol. 113, pp. 132–135, 2012.

[11] N. Basavegowda and Y. Rok Lee, "Synthesis of silver nanoparticles using Satsuma mandarin (*Citrus unshiu*) peel extract: A novel approach towards waste utilization," *Materials Letters*, vol. 109, no. 109, pp. 31–33, 2013.

[12] R. G. Roopan, Rohit, G. Madhumitha et al., "Low-cost and eco-friendly phyto-synthesis of silver nanoparticles using *Cocos nucifera* coir extract and its larvicidal activity," *Industrial Crops and Products*, vol. 43, pp. 631–635, 2013.

[13] A. Malhotra, N. Sharma, N. FNU et al., "Multi-analytical approach to understand biomineralization of gold using rice bran: a novel and economical route," *RSC Advances*, vol. 4, pp. 39484–39490, 2014.

[14] B. S. Harish, K. B. Uppuluri, and V. Anbazhagan, "Synthesis of fibrinolytic active silver nanoparticle using wheat bran xylan as a reducing and stabilizing agent," *Carbohydrate Polymers*, vol. 132, pp. 104–110, 2015.

[15] M. S. Jabir, Y. M. Saleh, G. M. Sulaiman et al., "Green synthesis of silver nanoparticles using *Annona muricata* extract as an inducer of apoptosis in cancer cells and inhibitor for NLRP3 inflammasome via enhanced autophagy," *Nanomaterials*, vol. 11, no. 2, p. 384, 2021.

[16] M. S. Jabir, A. A. Hussien, G. M. Sulaiman et al., "Green synthesis of silver nanoparticles from *Eriobotrya japonica* extract: a promising approach against cancer cells proliferation, inflammation, allergic disorders and phagocytosis induction," *Artificial cells, nanomedicine, and biotechnology*, vol. 49, no. 1, pp. 48–60, 2021.

[17] E. H. Endo, T. Ueda-Nakamura, and C. V. Nakamura, "Activity of spray-dried microparticles containing pomegranate peel extract against Candida albicans," *Molecules*, vol. 17, no. 9, pp. 10094–10107, 2012.

[18] T. Ismail, P. Sestili, and S. Akhtar, "Pomegranate peel and fruit extracts: a review of potential anti-inflammatory and anti-infective effects," *Journal of Ethnopharmacology*, vol. 143, no. 2, pp. 397–405, 2012.

[19] R. Habibipour, L. Moradi-Haghgou, and A. Farmany, "Green synthesis of AgNPs@PPE and its *Pseudomonas aeruginosa* biofilm formation activity compared to pomegranate peel extract," *International Journal of Nanomedicine*, vol. 14, pp. 6891–6899, 2019.

[20] M. A. El-Awady, N. S. Awad, and A. E. El-Tarras, "Evaluation of the anticancer activities of pomegranate (Punica granatum) and harmal (Rhazya stricta) plants grown in Saudi arabia," *International Journal of Current Microbiology and Applied Sciences*, vol. 4, pp. 1158–1167, 2015.

[21] A. Elkady, "Crude alkaloid extract of *Rhazya stricta* inhibits cell growth and sensitizes human lung cancer cells to cisplatin through induction of apoptosis," *Genetics and Molecular Biology*, vol. 36, no. 1, pp. 12–21, 2013.

[22] A. S. P. Moreira, F. M. Nunes, M. R. Domingues, and M. A. Coimbra, "Coffee melanoidins: structures, mechanisms of formation and potential health impacts," *Food & Function*, vol. 3, no. 9, pp. 903–915, 2012.

[23] I. Hečimović, A. Belščak-Cvitanović, D. Horžić, and D. Komes, "Comparative study of polyphenols and caffeine in different coffee varieties affected by the degree of roasting," *Food Chemistry*, vol. 129, no. 3, pp. 991–1000, 2011.

[24] D. Herawati, P. E. Giriwono, F. N. A. Dewi, T. Kashiwagi, and N. Andarwulan, "Critical roasting level determines bioactive content and antioxidant activity of Robusta coffee beans," *Food Science and Biotechnology*, vol. 28, no. 1, pp. 7–14, 2019.

[25] A. Zabaniotou and P. Kamaterou, "Food waste valorization advocating circular bioeconomy - a critical review of potentialities and perspectives of spent coffee grounds biorefinery," *Journal of Cleaner Production*, vol. 211, pp. 1553–1566, 2019.

[26] S. I. Mussatto, E. M. S. Machado, S. Martins, and J. A. Teixeira, "Production, composition, and application of coffee and its industrial Residues," *Food and Bioprocess Technology*, vol. 4, no. 5, pp. 661–672, 2011.

[27] S. Sunoqrot, E. al-Shalabi, A. G. al-Bakri et al., "Coffee bean polyphenols can form biocompatible template-free antioxidant nanoparticles with various sizes and distinct colors," *ACS Omega*, vol. 6, no. 4, pp. 2767–2776, 2021.

[28] S. Raja, V. Ramesh, and V. Thivaharan, "Green biosynthesis of silver nanoparticles using *Calliandra haematocephala* leaf extract, their antibacterial activity and hydrogen peroxide sensing capability," *Arabian Journal of Chemistry*, vol. 10, no. 2, pp. 253–261, 2017.

[29] J. Fang, C. Zhong, and R. Mu, "The study of deposited silver particulate films by simple method for efficient SERS," *Chemical Physics Letters*, vol. 401, no. 1-3, pp. 271–275, 2005.

[30] P. Mulvaney, "Surface plasmon spectroscopy of nanosized metal particles," *Langmuir*, vol. 12, no. 3, pp. 788–800, 1996.

[31] K. Anandalakshmi, J. Venugobal, and V. Ramasamy, "Characterization of silver nanoparticles by green synthesis method using *Pedalium murex* leaf extract and their antibacterial activity," *Applied Nanoscience*, vol. 6, no. 3, pp. 399–408, 2016.

[32] A. Henglein, "Physicochemical properties of small metal particles in solution: "microelectrode" reactions, chemisorption, composite metal particles, and the atom-to-metal transition," *Journal of Physical Chemistry*, vol. 97, no. 21, pp. 5457–5471, 1993.

[33] M. Sastry, V. Patil, and S. R. Sainkar, "Electrostatically controlled diffusion of carboxylic acid derivatized silver colloidal particles in thermally evaporated fatty amine films," *Journal of Physical Chemistry B*, vol. 102, no. 8, pp. 1404–1410, 1998.

[34] A. T. Saeb, A. S. Alshammari, H. al-Brahim, and K. A. al-Rubeaan, "Production of silver nanoparticles with strong and stable antimicrobial activity against highly pathogenic and multidrug resistant bacteria," *The Scientific World Journal*, vol. 2014, Article ID 704708, 9 pages, 2014.

[35] P. G. Saad, R. D. Castelino, V. Ravi, I. S. al-Amri, and S. A. Khan, "Green synthesis of silver nanoparticles using Omani pomegranate peel extract and two polyphenolic natural products: characterization and comparison of their antioxidant, antibacterial, and cytotoxic activities," *Beni-Suef University Journal of Basic and Applied Sciences*, vol. 10, no. 1, p. 29, 2021.

[36] A. Zuorro, G. Maffei, A. Iannone, and R. Lavecchia, "Production of silver nanoparticles by spent coffee grounds extracts," in *5th International Conference on Green Chemistry and Technology, 6th International Conference on Environmental Chemistry and Engineering*, vol. 3, Rome, Italy, 2017no. 2.

[37] S. S. Balu, C. Bhakat, and S. Harke, "Synthesis of silver nanoparticles by chemical reduction and their antimicrobial activity," *International Journal of Engineering Research & Technology (IJERT)*, vol. 1, no. 6, pp. 1–5, 2012.

[38] B. A. Lakkappa, S. C. Jasmith, and M. G. Prabhuodeyara, "Effect of concentration and pH on the size of silver nanoparticles synthesized by green chemistry," *Organic & Medicinal Chemistry International Journal*, vol. 3, no. 5, article 555622, 2017.

[39] S. Mukherjee, D. Chowdhury, R. Kotcherlakota et al., "Potential theranostics application of bio-synthesized silver nanoparticles (4-in-1 system)," *Theranostics*, vol. 4, no. 3, pp. 316–335, 2014.

[40] C. H. Vinay, P. Goudanavar, and A. Acharya, "Development and characterization of pomegranate and orange fruit peel extract based silver nanoparticles," *Journal of Manmohan Memorial Institute of Health Sciences*, vol. 4, no. 1, pp. 72–85, 2018.

[41] L. Panzella, P. Cerruti, P. Aprea et al., "Silver nanoparticles on hydrolyzed spent coffee grounds (HSCG) for green antibacterial devices," *Journal of Cleaner Production*, vol. 268, article 122352, 2020.

[42] N. M. al Sufyani, N. A. Hussien, and Y. M. Hawsawi, "Characterization and anticancer potential of silver nanoparticles biosynthesized from *Olea chrysophylla* and *Lavandula dentata* leaf extracts on HCT116 colon cancer cells," *Journal of Nanomaterials*, vol. 2019, Article ID 7361695, 9 pages, 2019.

[43] P. S. Yerragopu, S. Hiregoudar, U. Nidoni, K. T. Ramappa, A. G. Sreenivas, and S. R. Doddagoudar, "Chemical synthesis of silver nanoparticles using tri-sodium citrate, stability study and their characterization," *International Research Journal of Pure and Applied Chemistry*, vol. 21, no. 3, pp. 37–50, 2020.

[44] X. Liu, K. Shan, X. Shao et al., "Nanotoxic effects of silver nanoparticles on normal HEK-293 cells in comparison to cancerous HeLa cell line," *International Journal of Nanomedicine*, vol. 16, pp. 753–761, 2021.

[45] V. Kumar and S. K. Yadav, "Plant-mediated synthesis of silver and gold nanoparticles and their applications," *Journal of Chemical Technology and Biotechnology*, vol. 84, no. 2, pp. 151–157, 2009.

[46] V. S. Suvith and D. Philip, "Catalytic degradation of methylene blue using biosynthesized gold and silver nanoparticles," *Spectrochimica Acta. Part A, Molecular and Biomolecular Spectroscopy*, vol. 118, pp. 526–532, 2014.

[47] R. Haniea, "System Theory, Proton Stability, Double-Slit Experiment, and Cyclotron Physics," *Journal of Advances in Physics*, vol. 17, pp. 161–168, 2020.

[48] K. Jeeva, M. Thiyagarajan, V. Elangovan, N. Geetha, and P. Venkatachalam, "*Caesalpinia coriaria* leaf extracts mediated biosynthesis of metallic silver nanoparticles and their antibacterial activity against clinically isolated pathogens," *Industrial Crops and Products*, vol. 52, pp. 714–720, 2014.

[49] N. Prabhu, D. T. Raj, G. K. Yamuna, S. S. Ayisha, and I. D. Joseph Puspha, "Synthesis of silver phyto nanoparticles and their anti-bacterial efficacy," *Digest Journal of Nanomaterials & Biostructures (DJNB)*, vol. 5, pp. 185–189, 2010.

[50] S. S. Shankar, A. Rai, A. Ahmad, and M. Sastry, "Rapid synthesis of Au, Ag, and bimetallic Au core–Ag shell nanoparticles using Neem (*Azadirachta indica*) leaf broth," *Journal of colloid and interface science*, vol. 275, no. 2, pp. 496–502, 2004.

[51] M. Nasiriboroumand, M. Montazer, and H. Barani, "Preparation and characterization of biocompatible silver nanoparticles using pomegranate peel extract," *Journal of Photochemistry and Photobiology. B*, vol. 179, pp. 98–104, 2018.

[52] D. F. Barbin, A. L. D. M. Felicio, D. W. Sun, S. L. Nixdorf, and E. Y. Hirooka, "Application of infrared spectral techniques on quality and compositional attributes of coffee: an overview," *Food Research International*, vol. 61, pp. 23–32, 2014.

[53] H.-W. Chien, C.-J. Kuo, L.-H. Kao, G. Y. Lin, and P. Y. Chen, "Polysaccharidic spent coffee grounds for silver nanoparticle immobilization as a green and highly efficient biocide," *International journal of biological macromolecules*, vol. 140, no. 1, pp. 168–176, 2019.

[54] J. Singh, "Chemo-bio synthesis of silver nanoparticles," *Journal of Nanomedicine Research*, vol. 4, no. 3, article 00092, 2016.

[55] K. Ranoszek-Soliwoda, E. Tomaszewska, E. Socha et al., "The role of tannic acid and sodium citrate in the synthesis of silver nanoparticles," *Journal of Nanoparticle Research*, vol. 19, no. 8, p. 273, 2017.

[56] A. Rautela, J. Rani, and M. Debnath (Das), "Green synthesis of silver nanoparticles from *Tectona grandis* seeds extract: characterization and mechanism of antimicrobial action on different microorganisms," *Journal of Analytical Science and Technology*, vol. 10, no. 1, 2019.

[57] S. Shrivastava, T. Bera, A. Roy, G. Singh, P. Ramachandrarao, and D. Dash, "Characterization of enhanced antibacterial effects of novel silver nanoparticles," *Nanotechnology*, vol. 18, no. 22, article 225103, 2007.